Extracellular matrix viscoelasticity regulates TGFβ1-induced epithelial-mesenchymal transition and apoptosis via integrin linked kinase

Jessica L. Sacco[1], Zachary T. Vaneman[1], Esther W. Gomez[1,2*]

[1]Department of Chemical Engineering, The Pennsylvania State University, University Park, Pennsylvania, USA

[2]Department of Biomedical Engineering, The Pennsylvania State University, University Park, Pennsylvania, USA

*Corresponding author: ewg10@psu.edu

Keywords: epithelial cells, elasticity, hydrogels, transforming growth factor, disease progression, cell adhesion, viscous dissipation

Running title: Viscoelasticity regulates TGFβ1 signaling

Abstract

Transforming growth factor (TGF)-β1 is a multifunctional cytokine that plays important roles in health and disease. Previous studies have revealed that TGFβ1 activation, signaling, and downstream cell responses including epithelial-mesenchymal transition (EMT) and apoptosis are regulated by the elasticity or stiffness of the extracellular matrix. However, tissues within the body are not purely elastic, rather they are viscoelastic. How matrix viscoelasticity impacts cell fate decisions downstream of TGFβ1 remains unknown. Here, we synthesized polyacrylamide hydrogels that mimic the viscoelastic properties of breast tumor tissue. We found that increasing matrix viscous dissipation reduces TGFβ1-induced cell spreading, F-actin stress fiber formation, and EMT-associated gene expression changes, and promotes TGFβ1-induced apoptosis in mammary epithelial cells. Furthermore, TGFβ1-induced expression of integrin linked kinase (ILK) and colocalization of ILK with vinculin at cell adhesions is attenuated in mammary epithelial cells cultured on viscoelastic substrata in comparison to cells cultured on nearly elastic substrata. Overexpression of ILK promotes TGFβ1-induced EMT and reduces apoptosis in cells cultured on viscoelastic substrata, suggesting that ILK plays an important role in regulating cell fate downstream of TGFβ1 in response to matrix viscoelasticity.

Introduction

Transforming growth factor (TGF)-β1 is a multifunctional cytokine that is important for normal physiological processes (de Caestecker, 2004; Massagué, J., 1998), and when misregulated it can contribute to the progression of pathologies including cancer (Elliot & Blobe, 2005; Gordon & Blobe, 2008; Massagué, J, 2008; Sankhe, Sacco, & Gomez, 2023). TGFβ1 serves as a tumor suppressor in the early stages of tumorigenesis by promoting apoptosis and inhibiting proliferation of normal, pre-malignant cells (Derynck, Akhurst, & Balmain, 2001; Tang et al., 2003). As cancer progresses, TGFβ1 takes on a tumor promoter role where it facilitates epithelial-mesenchymal transition (EMT), cell invasion into the surrounding stroma, and metastasis (Ellenrieder et al., 2001; Kim et al., 2020; Morel et al., 2008). Factors that regulate the shift of TGFβ1 from a tumor suppressor to a tumor promoter role are not well understood.

The mechanical properties of tumors evolve during tumorigenesis and have been shown to regulate some aspects of cancer (Kumar & Weaver, 2009; Liu, Luo, Ju, & Song, 2020). For example, breast tissue significantly stiffens as breast cancer progresses (Levental et al., 2010; Lopez, Kang, You, McDonald, & Weaver, 2011; Plodinec et al., 2012) and this is accompanied by an increase in tissue viscosity (Levental et al., 2010; Siegmann et al., 2010; Sinkus et al., 2007). Many studies have demonstrated that matrix elasticity, or stiffness, impacts TGFβ1 signaling (Allen, Cooke, & Alliston, 2012; Brown, Fiore, Sulchek, & Barker, 2013; Giacomini, Travis, Kudo, & Sheppard, 2012; Pang, Mingshu et al., 2017; Wipff, Rifkin, Meister, & Hinz, 2007), EMT progression (Brown et al., 2013; Kilinc, Han, Barrett, Anandasivam, & Nelson, 2021; Leight, Wozniak, Chen, Lynch, & Chen, 2012; Lopez-Cavestany et al., 2023; Markowski, Brown, & Barker, 2012; McGrail, Kieu, & Dawson, 2014; O'Connor, Joseph, Riley, Nalluri, Ashar, & Gomez, 2015; Pang, Mingshu et al., 2017; Rice et al., 2017; Wei et al., 2015), and apoptosis (Kilinc et al., 2021; Leight et al., 2012; Sharma, Goswami, Zhang, & Rahama, 2018; Wang, Dembo, & Wang, 2000). However, tissues in our body are not purely elastic, they are viscoelastic, and the impact of matrix viscous dissipation on cells is less documented. Several recent studies have shown that culturing cells on viscoelastic substrata influences cell spreading, cytoskeletal organization, and focal adhesion formation (Charrier, Pogoda, Wells, & Janmey, 2018; Chaudhuri, Cooper-White, Janmey, Mooney, & Shenoy, 2020; Chaudhuri et al., 2015; Hui, Gimeno, Guan, & Caliari, 2019; Hui, Moretti, Barker, & Caliari, 2021). Focal adhesion formation and integrin engagement enable cells to sense and respond to mechanical changes in their environment and are particularly important for allowing cells to spread on viscoelastic materials (Gong et al., 2018). These factors also contribute to epithelial cell phenotypic changes implicated in disease progression. While the effect of matrix stiffness on cell behavior has been well studied, how matrix viscoelasticity impacts apoptosis and EMT downstream of TGFβ1 remains unclear.

Integrin linked kinase (ILK) plays an important role in cell mechanosensing and cell response to TGFβ1. ILK is an intracellular protein that localizes to focal adhesions and interacts with the actin cytoskeleton to facilitate communication between the cell and extracellular matrix (Li, Zhang, & Wu, 1999). Matrix stiffness, TGFβ signaling, and ILK have been shown to cooperatively influence

cell behavior. TGFβ1 upregulates ILK expression and ILK inhibition attenuates TGFβ1-induced EMT (Serrano, McDonald, & Dedhar, 2013). Mammary carcinoma cells exhibit increased ILK expression as matrix stiffness increases (Pang, MF et al., 2016). Furthermore, ILK mediates a matrix stiffness-induced switch in TGFβ1 function; ILK knockdown results in TGFβ1-induced apoptosis in cells cultured on both soft and stiff substrata (Kilinc et al., 2021). However, how matrix viscoelasticity regulates ILK signaling in the context of TGFβ1-induced EMT is not known.

Here, we synthesized a series of viscoelastic polyacrylamide hydrogels to examine how viscous dissipation impacts mammary epithelial cell response to TGFβ1. We held the storage modulus constant at 2000 Pa to mimic the elastic properties of breast tumors and varied the loss modulus to have substrata with varying levels of viscous dissipation. We find that culture of mammary epithelial cells on viscoelastic substrata reduces TGFβ1-induced cell spreading, elongation, stress fiber formation, and gene expression changes associated with EMT in comparison to what is observed in cells cultured on nearly elastic substrata with the same storage modulus. In addition, when cells are cultured on viscoelastic substrata, TGFβ1 induces higher levels of apoptosis in comparison to when cells are cultured on nearly elastic substrata. Furthermore, TGFβ1 induces increased expression of ILK in cells cultured on nearly elastic substrata but not in cells cultured on viscoelastic substrata. Overexpression of ILK promotes TGFβ1-induced EMT and reduces TGFβ1-induced apoptosis in cells cultured on viscoelastic substrata, suggesting that ILK plays an important role in mediating cell response to TGFβ1 and substratum viscoelasticity. These findings provide evidence that the viscous properties of the cellular microenvironment regulate cell fate downstream of TGFβ1 and that ILK plays a critical role in sensing the mechanical properties of the matrix.

Materials and methods

Viscoelastic polyacrylamide hydrogel synthesis

Polyacrylamide hydrogels with varying loss moduli were synthesized using an adapted protocol (Charrier et al., 2020). Briefly, the hydrogels were composed of an acrylamide monomer (Sigma Aldrich) and bis-acrylamide crosslinker (Sigma Aldrich) and the loss moduli were varied by trapping strands of linear acrylamide within the crosslinked polyacrylamide network. To make linear polyacrylamide, a solution of 5% acrylamide in water was mixed, degassed, and polymerized by adding 0.05% N,N,N',N'-tetramethylethylenediamine (TEMED) and 0.025% ammonium persulfate (APS). The solution was polymerized for 1 hour at 37 °C then stored at 4 °C in the dark. The concentrations of TEMED and APS were low to ensure that long linear chains of polyacrylamide were formed.

To form the activated crosslinked network, water, acrylamide, bis-acrylamide, and 4% N-hydroxysulfosuccinimide (NHS) dissolved in dimethyl sulfoxide (DMSO) were mixed according to the compositions described in Table S1 and the solution was degassed. A 1:10 v/v mixture of 4% NHS dissolved in DMSO and gel solution were mixed, and the amount of water in the solution was adjusted to compensate for the added NHS. To polymerize the network, 0.075% APS and 0.25% TEMED were added to the solution and thoroughly mixed. The solution was deposited onto

functionalized glass slides treated sequentially with 0.1 N NaOH (Sigma Aldrich), 2% v/v aminopropyltrimethoxysilane (APTMS; Sigma Aldrich) diluted in acetone, and 0.5% glutaraldehyde (Sigma Aldrich) diluted in 1× phosphate buffered saline (PBS). The solution was then covered with a Rain-X treated coverslip to obtain a flat hydrogel surface once polymerized. Hydrogels were polymerized for 15 minutes at room temperature. Then, the top coverslip was removed, and the hydrogels were covered in 0.5 M HEPES (pH 8.5) and sterilized in a CL-1000 Ultraviolet Crosslinker for 15 minutes. Immediately after sterilization, the hydrogels were covered with 0.1 μg/mL human fibronectin (BD Biosciences) and incubated overnight at 4 °C. Hydrogels were made fresh for each experiment and not stored.

Mechanical characterization of hydrogels

Rheology was performed using an RFS-3 rheometer (Rheometric Scientific Inc., Model number ARES-3). Immediately after polymerization initiation, the hydrogel solution was deposited into the cup of the rheometer. Time sweeps were performed at a frequency of 1 rad/s and 2% strain for about 30 minutes or until polymerization was complete, as indicated by a plateau in G' and G" values. Frequency sweeps were performed from 0.3-100 rad/s with 2% strain. The G' and G" values reported in Table S1 were measured at the frequency 1 rad/s, as it has been reported that cell mechanosensing occurs at this frequency (Charrier et al., 2018).

Cell culture

Normal murine mammary gland (NMuMG) epithelial cells (American Type Culture Collection ATCC CRL-1636) were authenticated by Genetica Cell Line Testing, a LabCorp brand, and cells tested negative for mycoplasma. NMuMG cells were grown in Dulbecco's Modified Eagle Medium (DMEM) with 10% (v/v) fetal bovine serum (FBS, Atlanta Biologicals), 0.01% gentamicin (Gibco), and 10 μg/mL insulin (Sigma Aldrich). Cells were cultured in medium in a 37 °C incubator with 5% CO_2. Prior to seeding cells onto the polyacrylamide hydrogels, media was added to the hydrogels so that hydrogels were hydrated. Following incubation of the hydrogels at 37 °C for 30 minutes, cells were then seeded onto the hydrogel surfaces at a density of 75,000 cells/cm^2. Cells were allowed to adhere to the hydrogel surfaces for 24 hours after seeding, followed by treatment with 10 ng/mL of recombinant human TGFβ1 (R&D Systems) or a vehicle control (1 mg/mL bovine serum albumin in 4 mM HCl) for 48 hours. For cleaved caspase-3 staining and caspase-3 activity experiments, TGFβ1 treatment was for 24 hours.

Plasmids and transfections

A plasmid encoding mouse EGFP-tagged integrin linked kinase (mILK-EGFP-N1) (Martin, Nava, Wickström, & Gräter, 2022) was obtained from Sara Wickström (Addgene plasmid #176896). The plasmid encoding the empty vector pEGFP-N1 was obtained from Gerard Elberg (Department of Pediatrics, The University of Oklahoma Health Sciences Center) (Elberg et al., 2008). Cells were transfected with the plasmids using Lipofectamine with Plus Reagent (Thermo) according to the manufacturer's protocol. Cells were seeded onto hydrogels 24 hours after transfection.

Immunofluorescence staining

For α smooth muscle actin (αSMA) staining, cells were fixed with ice cold 1:1 methanol/acetone for 10 minutes at -20 °C. For staining of E-cadherin and cleaved caspase-3, cells were fixed with 4% paraformaldehyde at room temperature for 15 minutes. Samples were permeabilized with 0.5% IGEPAL and 0.1% Triton X-100 diluted in 1× PBS for 10 minutes each at room temperature. The samples were incubated with a blocking buffer composed of 10% goat serum (Sigma Aldrich) diluted in 1× PBS for 1.5 hours at room temperature. Samples were then incubated with the following primary antibodies overnight at 4 °C: E-cadherin (1:200; 24E10; Cell Signaling Technologies; cat #: 3195), αSMA (1:200; 1A4; Sigma; cat #: A5228), and cleaved caspase-3 (1:400; Asp175; Cell Signaling Technologies; cat #: 9661). For vinculin and ILK co-staining, samples were incubated with ice cold cytoskeletal stabilization buffer (50 mM NaCl, 0.5% Triton X-100, 10 mM PIPES, 2.5 mM $MgCl_2$, 1 mM EGTA, and 0.3 M Sucrose in PBS) for 1 minute then fixed with 4% paraformaldehyde at room temperature for 15 minutes. Samples were incubated with a blocking buffer composed of 5% bovine serum albumin, 10% goat serum, and 0.1% Triton X-100 in PBS for 2 hours at room temperature and then simultaneously incubated with vinculin (1:200; Sigma; cat # V9131) and ILK1 (1:150; Cell Signaling Technologies; cat # 3862) primary antibodies overnight at 4 °C. Following incubation with primary antibodies, all samples were rinsed three times with 1× PBS with gentle shaking to remove unbound primary antibody and then incubated at room temperature for 1 hour with Alexa Fluor-conjugated secondary antibodies (1:500 or 1:1000 dilution, Life Technologies). For visualization of F-actin, cells were incubated with Alexa-Fluor 594 phalloidin (Thermo) according to the manufacturer's protocol. The cell nuclei were visualized by treatment with Hoechst 33342 (1:10,000; Life Technologies) at room temperature for 15 minutes. Samples were rinsed thoroughly with 1× PBS, and then mounted onto microscope slides with Fluoromount-G (Invitrogen) to prepare them for imaging.

Microscopy and image analysis

Samples mounted on microscope slides were imaged using a 20× or 40× objective on a Nikon Eclipse Ti-E inverted fluorescence microscope equipped with a Photometrics CoolSNAP HQ^2 CCD camera. ImageJ software was used to measure cell spread area and aspect ratio (major/minor axis) of the cells. Vinculin and ILK images were overlayed in ImageJ to visualize co-localization. Vinculin and ILK organization was then categorized as punctate, mixed, or diffuse and the percentage of cells showing these staining patterns is reported as a function of substratum viscoelasticity and treatment with TGFβ1.

Caspase-3 activity

Caspase-3 activity was determined using the EnzChek Caspase-3 Assay Kit #1 (Thermo). Briefly, cells were harvested from the hydrogels using trypsin then washed with 1× PBS. A hemocytometer was used to count the cells to ensure equal amounts of cells from each sample were used in the assay. The assay was carried out according to the manufacturer's instructions. The fluorescence was measured using a TECAN Infinite 200 Pro microplate reader with excitation/emission wavelengths of 342/441 nm.

Western blotting

Whole cell lysates were collected using RIPA buffer (Thermo) with protease and phosphatase inhibitors. Protein concentration was quantified using a Pierce BCA Protein Assay Kit (Thermo). Equal amounts of protein were separated on NuPAGE 4-12% Bis-Tris (Thermo) or NuPAGE 3-8% Tris-Acetate (Thermo) gels and transferred to polyvinyl difluoride (PVDF) or nitrocellulose membranes using an XCell SureLock Mini-Cell (Invitrogen). Membranes were blocked with 5% nonfat milk for an hour then incubated with the following primary antibodies overnight at 4 °C: E-cadherin (1:1000; clone: 24E10; Cell Signaling Technologies; cat # 3195), αSMA (1:1000; clone: 1A4; Sigma; cat #A5228), ILK1 (1:1000; Cell Signaling Technologies; cat # 3862), GAPDH (1:1000; clone: D16H11; Cell Signaling Technologies; cat # 5174), and α-tubulin (1:1000; clone: DM1A; Thermo; cat # 62204). Membranes were then incubated with IRDye secondary antibodies (1:10,000; Li-COR Biosciences; cat # 926-32210 and 925-68071) and imaged using a Li-COR Odyssey CLx imager. Densitometric analysis of the blots was performed with ImageJ software. Normalized protein expression was quantified by dividing the intensity of the bands for the target protein by the intensity of the bands of the loading control. Relative protein levels were determined by dividing the normalized intensity of each sample by the intensity of the control for each experiment.

Statistical analysis

At least three trials were performed for each experiment. Data are presented as mean ± standard error of the mean (s.e.m.). An analysis of variance followed by a Tukey-Kramer post hoc test using MATLAB was used to determine statistical differences. Differences were considered significant for $p<0.05$.

Results

Synthesis of viscoelastic hydrogels to mimic breast tumor mechanical properties

Soft tissues such as the mammary gland are viscoelastic and mechanical properties of these tissues can be described by a storage modulus (G'), a parameter indicative of material stiffness, and a loss modulus (G"), a parameter that gives information about the viscosity of the tissue (Chaudhuri et al., 2020). Healthy tissue has a loss modulus that is approximately 10% of its storage modulus (Chaudhuri et al., 2020) and it has been reported that breast tumors are more viscous than surrounding healthy breast tissue (Siegmann et al., 2010; Sinkus et al., 2007). We designed a series of polyacrylamide hydrogels with controlled elasticity and viscous dissipation to mimic breast tumor viscoelastic properties. Crosslinker and linear acrylamide concentrations were varied following a modified protocol (Charrier et al., 2020), to create hydrogels with defined G' and G" (Figure 1 and Table S1). Rheometry was used to characterize the mechanical properties of the hydrogels. During polymerization, G' and G" increase over time and then begin to plateau as the hydrogels polymerize (Figure 1a). The frequency dependence of G' and G" was measured over a range of 0.3-100 rad/s, and in this range G' is nearly constant (Figure 1b). Previous studies suggest that cell mechanosensing occurs at a frequency of 1 rad/s (Charrier et al., 2018), therefore, we

report values of G' and G" measured at 1 rad/s (0.16 Hz). For this study, we utilize hydrogels with G' of approximately 2000 Pa (Figure 1c and Table S1) and varying G" between 16 and 410 Pa (Figure 1d). The Young's modulus (E) can be determined from the storage modulus using $E = 2G'(1 + \vartheta)$ where ϑ is the Poisson ratio. Assuming a Poisson ratio of 0.5, the Young's modulus for the 0% linear acrylamide composition, which exhibits nearly elastic behavior, is 5700 Pa, which is comparable to the stiffness of malignant human breast tumors (Plodinec et al., 2012). Fibronectin was coupled to the hydrogels using NHS to enable cell adhesion to the hydrogels. Immunofluorescence microscopy revealed that fibronectin couples uniformly to hydrogel surfaces and the relative level of fibronectin attached and the number of cells attached to different hydrogel compositions is not statistically different (Figure S1a-c). This hydrogel system enables studying how the loss modulus impacts mammary cell response to TGFβ1.

Substratum viscous dissipation regulates TGFβ1-induced changes in cell morphology and cytoskeletal organization

During TGFβ1-induced EMT, cells undergo significant morphological changes including increased spreading and elongation (Nelson, Khauv, Bissell, & Radisky, 2008; O'Connor, JW & Gomez, 2013). Furthermore, studies have shown that blocking the ability of cells to spread attenuates TGFβ1-induced expression of some mesenchymal protein markers (O'Connor, JW & Gomez, 2013). To examine the impact of matrix viscous dissipation on cell morphology in response to TGFβ1, normal murine mammary gland (NMuMG) cells were cultured on fibronectin-coated viscoelastic hydrogels with fixed G' (2000 Pa) and varying G'' (16, 190, and 410 Pa) and treated with TGFβ1 or a control vehicle. Phase contrast microscopy images reveal that TGFβ1 treatment significantly increases cell spread area and aspect ratio compared to control vehicle treatment in cells cultured on nearly elastic substrata (G" = 16 Pa) (Figure 2a,c,d). Cells cultured on the viscoelastic substrata (G" = 190 or 410 Pa) have reduced cell spreading compared to cells cultured on the nearly elastic substrata following treatment with TGFβ1. These data suggest that matrix viscous dissipation impacts the ability of cells to undergo morphological changes in response to TGFβ1.

In addition to inducing cell shape changes, TGFβ1 promotes rearrangements of the cytoskeleton in epithelial cells, including stress fiber formation (Bhowmick et al., 2001; Haynes, Srivastava, Madson, Wittmann, & Barber, 2011; Nalluri, O'Connor, & Gomez, 2015). Previous studies have shown that matrix viscoelasticity can impact cytoskeletal organization and stress fiber formation (Charrier et al., 2018; Chaudhuri et al., 2015; Hui et al., 2021; Marozas, Anseth, & Cooper-White, 2019). Thus, we hypothesized that matrix viscoelasticity may regulate cytoskeletal structure in response to TGFβ1. Cytoskeletal remodeling was monitored using fluorescently tagged phalloidin to visualize filamentous (F)-actin (Figure 2b, Figure S2). In cells cultured on the nearly elastic substrata, TGFβ1 treatment promotes F-actin stress fiber formation, while cells treated with the control vehicle exhibit a cortical F-actin structure. Cells cultured on the viscoelastic substrata, regardless of treatment condition, have reduced formation of stress fibers compared to cells treated

with TGFβ1 that are cultured on nearly elastic substrata. These results suggest that substratum viscous dissipation impacts cytoskeletal reorganization in response to TGFβ1.

Increasing substratum viscous dissipation attenuates TGFβ1-induced changes in EMT-associated gene expression

TGFβ1-induced EMT is characterized by a downregulation in epithelial genes, such as E-cadherin, and an upregulation in mesenchymal genes, such as α smooth muscle actin (αSMA) (Kalluri & Weinberg, 2010). We examined the effect of substratum viscous dissipation on gene expression by monitoring E-cadherin and αSMA levels using immunofluorescence staining and western blotting. E-cadherin localizes to cell-cell junctions in control and TGFβ1-treated cells cultured on viscoelastic substrata and in control-treated cells cultured on nearly elastic substrata (Figure 3a). TGFβ1 treatment reduces E-cadherin expression and significantly increases the percentage of cells expressing αSMA on nearly elastic substrata (Figure 3a,b). In contrast, cells cultured on viscoelastic substrata do not show increased expression of αSMA in response to TGFβ1. Consistent with immunofluorescence staining, western blotting revealed that TGFβ1 treatment significantly reduces E-cadherin protein levels and significantly increases αSMA protein levels in cells cultured on nearly elastic substrata (Figure 3c-e). Conversely, cells cultured on viscoelastic substrata do not show gains in αSMA expression in response to TGFβ1 (Figure 3e). E-cadherin and αSMA protein levels do not change significantly in control-treated cells cultured on substrata as a function of varying loss moduli (Figure 3d,e). Furthermore, expression of E-cadherin is not downregulated in cells cultured on hydrogels with a loss modulus of 410 Pa following treatment with TGFβ1 (Figure 3d). These findings suggest that increasing viscous dissipation blocks TGFβ1-induced changes in the expression of some epithelial and mesenchymal markers.

Increasing substratum viscous dissipation promotes TGFβ1-induced apoptosis

Previous studies have shown that TGFβ1 induces EMT in mammary epithelial cells cultured on stiff elastic substrata but induces apoptosis in cells cultured on soft elastic substrata (Leight et al., 2012). To examine the impact of matrix viscoelasticity on TGFβ1-induced apoptosis, we monitored apoptosis by staining for cleaved caspase-3 and measuring caspase-3 activity. Immunofluorescence images reveal that in control vehicle treated cells, the percentage of cells staining for cleaved caspase-3 increases with increasing substratum viscous dissipation, though not significantly (Figure 4a,b). TGFβ1 treatment slightly increases the percentage of cells expressing cleaved caspase-3 when cells are cultured on nearly elastic substrata. In contrast, TGFβ1 treatment significantly increases the percentage of cells staining positive for cleaved caspase-3 when cells are cultured on viscoelastic substrata compared to control vehicle treated cells cultured on all substrata and compared to TGFβ1 treated cells cultured on nearly elastic substrata (Figure 4a,b). Consistent with the cleaved caspase-3 staining results, TGFβ1 treatment significantly increases caspase-3 activity in cells cultured on viscoelastic substrata compared to cells cultured on nearly elastic substrata (Figure 4c). Caspase-3 activity does not vary in control vehicle treated cells as a function of loss moduli. Taken together, these observations demonstrate

that TGFβ1 promotes apoptosis in cells cultured on substrata with a storage modulus of 2000 Pa when the substrata also exhibit viscous dissipation.

ILK mediates cell response to TGFβ1 and substratum viscoelasticity

ILK plays an important role in transducing mechanical signals from the cellular microenvironment into biophysical responses. Previous findings show that ILK knockdown results in TGFβ1-induced apoptosis in cells cultured on both soft and stiff elastic substrata, suggesting that ILK may regulate cell response to TGFβ1 and matrix elasticity (Kilinc et al., 2021). Thus, we hypothesized that ILK may mediate the differential EMT and apoptotic responses of cells to TGFβ1 and substratum viscoelasticity. Western blotting revealed that TGFβ1 treatment significantly increases ILK levels in cells cultured on nearly elastic substrata, while TGFβ1 treatment does not significantly increase ILK levels in cells cultured on substrata with increased viscous dissipation (Figure 5a,b). ILK protein levels do not change in control vehicle treated cells cultured on substrata with a storage modulus of 2000 Pa as a function of loss moduli. These findings suggest that the expression of ILK is regulated by TGFβ1 and matrix viscoelasticity.

Given that ILK is an important component of focal adhesions and facilitates cell-extracellular matrix signaling (Li et al., 1999), we sought to determine whether matrix viscoelasticity and TGFβ1 mediate localization of ILK to cell-matrix adhesions. Immunofluorescence staining for vinculin and ILK was used to monitor focal adhesion organization as a function of matrix viscous dissipation (Figure 5c). In cells cultured on nearly elastic substrata, vinculin and ILK localize to puncta in response to TGFβ1 treatment (Figure 5c,d). In contrast, cells treated with control vehicle show diffuse staining or a mixture of punctate and diffuse staining for vinculin and ILK. In cells cultured on substrata with increasing viscous dissipation, vinculin and ILK staining is mainly diffuse with a small percentage of cells showing mixed punctate and diffuse organization, regardless of treatment condition. For substrata with a loss modulus of 410 Pa, there is a slightly, though not significant, higher percentage of cells with diffuse vinculin and ILK staining compared to cells cultured on substrata with a loss modulus of 190 Pa, regardless of treatment condition (Figure 5c,d). Importantly, vinculin and ILK are co-localized, indicated by the yellow color in the merged images in Figure 5c. These results suggest that cell adhesive structures are regulated by TGFβ1 and matrix viscoelasticity.

To determine whether ILK expression is sufficient to promote EMT and block apoptosis in cells cultured on viscoelastic substrata in response to TGFβ1, we transfected cells with an ILK-GFP construct or with a GFP plasmid as a control. Overexpression of ILK-GFP was confirmed by fluorescence microscopy and western blotting (Figure S3a-c). In cells cultured on viscoelastic substrata with a storage modulus of 2000 Pa and loss modulus of 410 Pa, ILK overexpression increases cell spreading compared to cells transfected with the GFP control plasmid, and TGFβ1 significantly amplifies this increase (Figure 6a,b). Cell aspect ratio also increases in ILK-overexpressing cells compared to cells transfected with the GFP control plasmid when cultured on the viscoelastic substrata with a storage modulus of 2000 Pa and a loss modulus of 410 Pa, and TGFβ1-treatment augments this increase (Figure 6a,c).

Given that ILK plays an important role in TGFβ1-induced EMT (Serrano et al., 2013) and overexpression of ILK restores TGFβ1-induced cell spreading and elongation on viscoelastic substrata, we posited that ILK overexpression may enable TGFβ1 to induce EMT when cells are cultured on viscoelastic substrata. Western blotting revealed that for cells cultured on nearly elastic substrata (G" = 16 Pa), TGFβ1 treatment significantly reduces E-cadherin protein levels and increases αSMA protein levels compared to control vehicle treatment in both GFP and ILK-GFP transfected cells (Figure 6d-f). For cells cultured on viscoelastic substrata (G" = 410 Pa), TGFβ1 treatment decreases E-cadherin protein levels and significantly increases αSMA protein levels in ILK-GFP transfected cells, but GFP transfected cells are refractive to TGFβ1-induced changes in EMT markers. Together, these results suggest that ILK overexpression promotes changes in some EMT associated proteins in response to TGFβ1 when cells are cultured on viscoelastic substrata.

Matrix elasticity and ILK regulate a switch between TGFβ1-induced EMT and apoptosis (Kilinc et al., 2021). We determined that ILK overexpression rescues the ability of TGFβ1 to induce EMT on viscoelastic substrata, thus we hypothesized that ILK overexpression would also reduce TGFβ1-induced apoptosis on viscoelastic substrata. We find that caspase-3 activity remains low in cells cultured on nearly elastic substrata across all treatment conditions (Figure 6g). For cells cultured on viscoelastic substrata, TGFβ1 treatment increases caspase-3 activity in GFP-transfected cells compared to control vehicle-treated cells and compared to cells cultured on nearly elastic substrata across all treatment conditions. ILK overexpressing cells cultured on viscoelastic substrata do not exhibit an increase in caspase-3 activity levels with TGFβ1 treatment, but rather show similar caspase-3 activity to cells cultured on nearly elastic substrata for both TGFβ1 and control vehicle treatments. These findings provide support that ILK overexpression attenuates TGFβ1-induced apoptosis in cells cultured on viscoelastic substrata mimicking breast tumor mechanical properties.

Discussion

In this study, we found that substratum viscous dissipation regulates cell response downstream of TGFβ1 via ILK. Using an established protocol (Charrier et al., 2020), we synthesized polyacrylamide hydrogels with storage and loss moduli similar to diseased breast tissue and utilized the hydrogels to examine the impact of viscous dissipation on cell response to TGFβ1. In NMuMG epithelial cells cultured on nearly elastic substrata, TGFβ1 treatment induces cell spreading and elongation, F-actin stress fiber formation, and a decrease in E-cadherin and a gain in αSMA expression, suggesting that these cells undergo EMT. In contrast, cells cultured on viscoelastic substrata and treated with TGFβ1 maintain a rounded morphology. high E-cadherin levels, and low αSMA levels. Furthermore, TGFβ1 treatment increases cleaved caspase-3 levels and caspase-3 activity in cells cultured on viscoelastic substrata, suggesting that increasing substrate viscous dissipation blocks TGFβ1-induced EMT and promotes TGFβ1-induced apoptosis. TGFβ1 treatment also increases ILK levels in cells cultured on nearly elastic substrata but does not affect ILK levels in cells cultured on viscoelastic substrata. Furthermore, TGFβ1 promotes punctate focal adhesion organization in cells cultured on nearly elastic substrata, where

vinculin and ILK are co-localized. ILK overexpression reduces TGFβ1-induced apoptosis and promotes TGFβ1-induced EMT in cells cultured on viscoelastic substrata, indicating that ILK plays an important role in mediating cell response to substratum viscoelasticity downstream of TGFβ1.

Several recent studies have examined the impact of matrix viscous dissipation on cell morphology and actin polymerization. U2OS human bone osteosarcoma epithelial cells, LX-2 hepatic stellate cells, human lung fibroblasts, and NIH3T3 fibroblasts exhibit a decrease in cell spreading on viscoelastic hydrogels in comparison to on nearly elastic hydrogels when the storage moduli or Young's moduli are high (Chaudhuri et al., 2015; Hui et al., 2019; Hui et al., 2021; Marozas et al., 2019). Computational modeling results suggest that substratum viscosity suppresses cell spreading when cells are cultured on substrata with high stiffness, as observed in the abovementioned experiments (Gong et al., 2018). Our results for control vehicle treated cells are consistent with these previous studies as we find that mammary epithelial cells spread less when cultured on viscoelastic hydrogels than on nearly elastic hydrogels when the storage modulus is fixed to 2000 Pa. In addition, for hepatic stellate cells and fibroblasts, more actin stress fibers have been observed in cells cultured on nearly elastic substrata compared to viscoelastic substrata when the Young's modulus and storage modulus are high (E = 9 kPa and G'=5 kPa, respectively) (Chaudhuri et al., 2015; Hui et al., 2021). Here, we find that mammary epithelial cells cultured on hydrogels with a storage modulus of 2000 Pa have decreased F-actin stress fiber formation as viscous dissipation increases. Moreover, we find that mammary epithelial cells exhibit changes in cell area, aspect ratio, and cytoskeletal organization in response to TGFβ1 when cultured on nearly elastic hydrogels but not when cultured on viscoelastic hydrogels. These experiments provide new insights into how viscous dissipation impacts cell morphology and cytoskeletal organization in response to growth factors.

While many of the aforementioned studies found that increasing substratum viscoelasticity decreases cell spreading and elongation at higher stiffness, the opposite trend has been observed in some studies when cells are cultured on hydrogels with lower stiffness. For osteosarcoma and fibroblasts, cell spreading, actin stress fiber formation, and focal adhesion formation increase on viscoelastic substrata compared to nearly elastic substrata when the Young's modulus is low (1.4 kPa) (Chaudhuri et al., 2015; Gong et al., 2018). Spreading was higher in LX-2 hepatic stellate cells cultured on nearly elastic hydrogels compared to viscoelastic hydrogels of the same "stiff" storage modulus of 5000 Pa, but cell spreading and elongation did not significantly change in cells cultured on viscoelastic hydrogels in comparison to nearly elastic hydrogels of the same "soft" storage modulus of 500 Pa (Hui et al., 2019). Furthermore, it has been suggested that fibroblast migration and correlated movement of epithelial sheets depend on the ratio of G' to G" (Chester, Kathard, Nortey, Nellenbach, & Brown, 2018; Murrell, Kamm, & Matsudaira, 2011). However, another study found no correlation between the ratio of G' to G" and cell spreading (Chaudhuri et al., 2015). Future work should aim to understand how viscous dissipation impacts cell behaviors, including EMT and apoptosis, over a range of elastic moduli. These efforts would help to elucidate

whether the balance between elastic and viscous properties of the matrix is an important factor in regulating epithelial cell response to growth factors.

EMT is characterized by the downregulation of epithelial markers such as E-cadherin and the upregulation of mesenchymal markers including αSMA, vimentin, and N-cadherin. Recent studies have examined αSMA stress fiber organization in response to substrate viscoelasticity, though not in response to TGFβ1. The organization of αSMA stress fibers was reduced in stellate cells when cultured on viscoelastic polyacrylamide or hyaluronic acid hydrogels compared to when cultured on nearly elastic hydrogels of the same storage modulus (G' = 5000 Pa) (Charrier et al., 2018; Hui et al., 2019). Madin-Darby canine kidney (MDCK) epithelial cells cultured on P(CL-co-DLLA) hydrogels with an elastic modulus of 5 MPa and varying relaxation times had significantly higher mRNA levels of the mesenchymal marker N-cadherin as relaxation time increased and had no significant change in the levels of the epithelial marker E-cadherin (Chinghsuan Chang, Uto, Abdellatef, & Nakanishi, 2022). In spheroid models, cells grown in viscoelastic matrices have higher expression of mesenchymal genes compared to when grown in nearly elastic matrices. In one study, PANC-1 human pancreatic cancer cells encapsulated in viscoelastic phenylboronic acid containing polymers had an increase (all less than 2-fold) in N-cadherin, vimentin, Snail and Zeb1 mRNA levels compared to cells cultured within nearly elastic hydrogels of the same storage modulus (G' = 6000 Pa) (Lin, Chang, Nguyen, Fishel, & Lin, 2023). Interestingly, there was an almost four-fold increase in E-cadherin mRNA levels in cells cultured in viscoelastic compared to nearly elastic hydrogels (Lin et al., 2023). In another recent study, MCF10A human mammary epithelial cell spheroids were able to branch when grown in 3D viscoelastic alginate hydrogels and cells at the ends of branches had increased vimentin expression compared to cells grown in nearly elastic hydrogels of the same storage modulus (G' = 5000 Pa) (Elosegui-Artola et al., 2022). In our study, we find that TGFβ1 promotes a decrease in the expression of the epithelial marker E-cadherin and an increase in the expression of the mesenchymal marker αSMA in cells cultured on nearly elastic hydrogels, but cells cultured on viscoelastic hydrogels are refractive to TGFβ1-induced changes in these markers. Differences in the regulation of epithelial and mesenchymal proteins in these studies may arise from differences in cell type, growth factor treatment conditions, the elastic modulus of the matrix, or matrix dimensionality. Here, we use an elastic modulus that mimics that of a breast tumor (G' = 2000 Pa), while the previous studies highlighted utilize matrices with elastic moduli ranging from 5000 Pa to 5 MPa, all of which are more than two-fold greater in magnitude than that of normal mammary tissue and breast tumors. More research is needed to understand how matrix viscous dissipation regulates gene expression downstream of TGFβ1 and how cell type, matrix viscoelasticity, and matrix dimension play a role in this regulation.

Microenvironmental cues, such as matrix elasticity, have also been shown to regulate apoptosis. For example, A549 lung cancer cells, MDA-MB-231 breast cancer cells, and NIH3T3 fibroblasts undergo apoptosis more readily on low elastic modulus hydrogels than when cultured on hydrogels with a higher elastic modulus (Tilghman et al., 2010; Wang et al., 2000). Previous studies have also demonstrated that matrix elasticity can regulate apoptosis in response to TGFβ1. Upon TGFβ1

stimulation, NMuMG and MDCK epithelial cells undergo apoptosis when cultured on polyacrylamide hydrogels with a Young's modulus of 400 Pa but undergo EMT when cultured on stiffer polyacrylamide hydrogels with a Young's modulus greater than 8000 Pa (Leight et al., 2012). Regulation of apoptosis by matrix viscoelasticity is less investigated, but some recent studies demonstrate that matrix stress relaxation can impact apoptosis in stem cells. Mesenchymal stem cells cultured in 3D viscoelastic collagen matrices with an initial elastic modulus of 3000 Pa and varying stress relaxation times undergo increased apoptosis when cultured in slow-relaxing matrices compared to cells cultured in fast-relaxing matrices (Huang et al., 2023). In another study, human induced pluripotent stem cells (hiPSCs) were encapsulated in 3D viscoelastic alginate matrices with varying stress relaxation times (Indana, Agarwal, Bhutani, & Chaudhuri, 2021). Cells cultured in slow-relaxing hydrogels with low ligand density had higher levels of apoptosis than cells cultured in fast-relaxing hydrogels. Surprisingly, in this system, there was no difference in apoptosis levels in cells cultured in viscoelastic hydrogels with an initial elastic modulus of 3000 Pa compared to 20,000 Pa with similar relaxation times (Indana et al., 2021). In our studies, we find that when the loss modulus of the matrix is increased by embedding linear polyacrylamide within the hydrogel, cells cultured on the hydrogels exhibit higher levels of apoptosis in response to TGFβ1. Future work should aim to further understand how matrix viscous dissipation influences apoptosis in response to growth factors.

To elucidate mechanistically how matrix viscoelasticity mediates cell response to TGFβ1, we investigated the impact of viscous dissipation on ILK expression. ILK is a critical regulator of focal adhesion dynamics and stability and it provides a link between the actin cytoskeleton and integrin-mediated adhesion sites (Zervas, Chen, Guo, & Wu, 2001). Previous studies have demonstrated that deficiency of ILK can lead to disrupted focal adhesion maturation and actin remodeling (Stanchi et al., 2009) and point mutations to the ATP binding domain of ILK reduce cell traction and migration (Martin et al., 2022). Furthermore, downregulation of ILK has been shown to reduce spreading in mammary epithelial cells cultured on stiff elastic substrata (Han, Pang, & Nelson, 2018) and ILK knockdown promotes TGFβ1-induced apoptosis instead of EMT in cells cultured on stiff elastic substrata (Kilinc et al., 2021). In our study, we found that mammary epithelial cells increase the expression of ILK in response to TGFβ1 treatment when cultured on nearly elastic hydrogels but not when cultured on viscoelastic hydrogels with the same storage modulus. We found that in cells cultured on nearly elastic substrata, TGFβ1 promotes punctate focal adhesion organization with co-localization of vinculin and ILK at focal adhesion sites. In contrast, when viscous dissipation of the hydrogel is increased cells show a mixture of punctate and diffuse staining for vinculin and ILK. In addition, we found that overexpression of ILK increases cell spreading and promotes TGFβ1-induced EMT and abrogates TGFβ1-induced apoptosis in cells cultured on viscoelastic substrates with a storage modulus of 2000 Pa. These results suggest that by increasing ILK expression, focal adhesion formation and maturation may allow for cell spreading and EMT induction by TGFβ1. Future work should aim to understand how matrix viscoelasticity influences integrin engagement and focal adhesion properties downstream of TGFβ1 to regulate cell spreading and cell fate.

Acknowledgements

The authors would like to thank Dr. Justin Brown for use of the LI-COR Odyssey Imaging System for western blot imaging, Dr. Andrew Zydney for use of the TECAN Infinite 200 Pro microplate reader for protein quantification, Dr. Enrique Gomez for use of the RFS-3 rheometer for characterization of hydrogel mechanical properties, and Dr. Spencer Szczesny for helpful discussions. This work was supported by the National Science Foundation (CMMI-1751785 to EWG), NASA PSGC (JLS), and the Penn State Department of Chemical Engineering Biofellowship (ZTV).

Author Contributions

J.L.S., Z.T.V., and E.W.G. designed the experiments. J.L.S. and Z.T.V. performed experiments. J.L.S., Z.T.V., and E.W.G. contributed to data analysis and wrote the manuscript.

Conflict of Interest

No conflict of interest is declared

Data Availability

The data that support the findings of this study are available from the corresponding author upon reasonable request.

References

Allen, J. L., Cooke, M. E., & Alliston, T. (2012). ECM stiffness primes the TGFbeta pathway to promote chondrocyte differentiation. *Mol Biol Cell, 23*(18), 3731-3742. doi:10.1091/mbc.E12-03-0172

Bhowmick, N., Ghiassi, M., Bakin, A., Aakre, M., Lundquist, C., Engel, M., . . . Moses, H. (2001). Transforming Growth Factor-β1 Mediates Epithelial to Mesenchymal Transdifferentiation through a RhoA dependent Mechanism. *Molecular Biology of the Cell, 12*, 27-36.

Brown, A. C., Fiore, V. F., Sulchek, T. A., & Barker, T. H. (2013). Physical and chemical microenvironmental cues orthogonally control the degree and duration of fibrosis-associated epithelial-to-mesenchymal transitions. *J Pathol, 229*(1), 25-35. doi:10.1002/path.4114

Charrier, E. E., Pogoda, K., Li, R., Park, C. Y., Fredberg, J. J., & Janmey, P. A. (2020). A novel method to make viscoelastic polyacrylamide gels for cell culture and traction force microscopy. *APL Bioengineering, 4*(3), 036104.

Charrier, E. E., Pogoda, K., Wells, R. G., & Janmey, P. A. (2018). Control of cell morphology and differentiation by substrates with independently tunable elasticity and viscous dissipation. *Nature Communications, 9*.

Chaudhuri, O., Cooper-White, J., Janmey, P. A., Mooney, D. J., & Shenoy, V. B. (2020). Effects of extracellular matrix viscoelasticity on cellular behaviour. *Nature, 584*, 535-546.

Chaudhuri, O., Gu, L., Darnell, M., Klumpers, D., Bencherif, S. A., Weaver, J. C., . . . Mooney, D. J. (2015). Substrate stress relaxation regulates cell spreading. *Nature Communications, 6*(6364).

Chester, D., Kathard, R., Nortey, J., Nellenbach, K., & Brown, A. (2018). Viscoelastic properties of microgel thin films control fibroblast modes of migration and pro-fibrotic responses. *Biomaterials, 185*, 371-382.

Chinghsuan Chang, A., Uto, K., Abdellatef, S. A., & Nakanishi, J. (2022). Precise Tuning and Characterization of Viscoelastic Interfaces for the Study of Early Epithelial-Mesenchymal Transition Behaviors. *Langmuir, 38*, 5307-5314.

de Caestecker, M. (2004). The transforming growth factor-β superfamily of receptors. *Cytokine and Growth Factor Reviews, 15*, 1-11.

Derynck, R., Akhurst, R., & Balmain, A. (2001). TGF-β signaling in tumor suppression and cancer progression. *Nature Genetics, 29*, 117-129.

Elberg, G., Chen, L., Elberg, D., Chan, M., Logan, C., & MA, T. (2008). MKL1 mediates TGF-β1-induced α-smooth muscle actin expression in human renal epithelial cells. *American Journal of Physiology Renal Physiology, 294*, F1116-F1128.

Ellenrieder, V., Hendler, S., Boeck, W., Seufferlein, T., Menke, A., Ruhland, C., . . . Gress, T. (2001). Transforming growth factor β1 treatment leads to an epithelial-mesenchymal transdifferentiation of pancreatic cancer cells requiring extracellular signal-regulated kinase 2 activation. *Cancer Research, 61*(10), 4222-4228.

Elliot, R., & Blobe, G. (2005). Role of transforming growth factor Beta in human cancer. *J. Clin. Oncol., 23*(9), 2078-2093.

Elosegui-Artola, A., Gupta, A., Najibi, A. J., Ri Seo, B., Garry, R., Tringides, C. M., . . . Mooney, D. J. (2022). Matrix viscoelasticity controls spatiotemporal tissue organization. *nature materials, 22*, 117-127.

Giacomini, M. M., Travis, M. A., Kudo, M., & Sheppard, D. (2012). Epithelial cells utilize cortical actin/myosin to activate latent TGF-beta through integrin alpha(v)beta(6)-dependent physical force. *Exp Cell Res, 318*(6), 716-722. doi:10.1016/j.yexcr.2012.01.020

Gong, Z., Szczesny, S. E., Caliari, S. R., Charrier, E. E., Chaudhuri, O., Cao, X., . . . Shenoy, V. B. (2018). Matching material and cellular timescales maximizes cell spreading on viscoelastic substrates. *Proceedings of the National Academy of the Sciences of the United States of America, 115*, E2686-E2695.

Gordon, K., & Blobe, G. (2008). Role of transforming growth factor-β superfamily signaling pathways in human disease. *Biochimica et Biophysica Acta (BBA)- Molecular Basis of Disease, 1782*(4), 197-228.

Han, S., Pang, M., & Nelson, C. (2018). Substratum stiffness tunes proliferation downstream of Wnt3a in part by regulating integrin-linked kinase and frizzled-1. *Journal of Cell Science, 131*.

Haynes, J., Srivastava, J., Madson, N., Wittmann, T., & Barber, D. L. (2011). Dynamic actin remodeling during epithelial-mesenchymal transition depends on increased moesin expression. *Mol Biol Cell, 22*(24), 4750-4764. doi:10.1091/mbc.E11-02-0119

Huang, D., Li, Y., Ma, Z., Lin, H., Zhu, Z., Xiao, Y., & Zhang, X. (2023). Collagen hydrogel viscoelasticity regulates MSC chondrogenesis in a ROCK-dependent manner. *Science Advances, 9*(6), eade9497.

Hui, E., Gimeno, K., Guan, G., & Caliari, S. (2019). Spatiotemporal control of viscoelasticity in phototunable hyaluronic acid hydrogels. *Biomacromolecules, 20*, 4126-4134.

Hui, E., Moretti, L., Barker, T., & Caliari, S. (2021). Combined influence of viscoelastic and adhesive cues on fibroblast spreading and focal adhesion organization. *Cellular and Molecular Bioengineering, 14*(5), 427-440.

Indana, D., Agarwal, P., Bhutani, N., & Chaudhuri, O. (2021). Viscoelasticity and adhesion signaling in biomaterials control human pluripotent stem cell morphogenesis in 3D culture. *Advanced Materials, 33*(43), 2101966.

Kalluri, R., & Weinberg, R. (2010). The Basics of Epithelial-Mesenchymal Transition. *J. Clin. Invest., 120*.

Kilinc, A., Han, S., Barrett, L., Anandasivam, N., & Nelson, C. (2021). Integrin-linked kinase tunes cell–cell and cell matrix adhesions to regulate the switch between apoptosis and EMT downstream of TGFβ1. *Mol. Biol. Cell, 32*(5), 402-412.

Kim, B., Ahn, D., Kang, N., Yeo, C., Kim, Y., & Lee, K. (2020). TGF-β induced EMT and stemness characteristics are associated with epigenetic regulation in lung cancer. *Scientific Reports, 10*(1), 10597.

Kumar, S., & Weaver, V. (2009). Mechanics, malignancy, and metastasis: the force journey of a tumor cell. *Cancer Metastasis Rev, 28*(1-2), 113-127.

Leight, J., Wozniak, M., Chen, S., Lynch, M., & Chen, C. (2012). Matrix rigidity regulates a switch between TGFβ1-induced apoptosis and epithelial-mesenchymal transition. *Molecular Biology of the Cell, 23*(5).

Levental, I., Levental, K., Klein, E., Assoian, R., Miller, R., Wells, R., & Janmey, P. (2010). A simple indentation device for measuring micrometer-scale tissue stiffness. *J. Phys. Condens. Matter, 22*, 194120.

Li, F., Zhang, Y., & Wu, C. (1999). Integrin linked kinase is localized to cell-matrix focal adhesions but not cell-cell adhesion sites and the focal adhesion localization of integrin

linked kinase is regulated by the PINCH-binding ANK repeats. *Journal of Cell Science, 112*(24), 4589-4599.

Lin, F., Chang, C., Nguyen, H., Fishel, M., & Lin, C. (2023). Viscoelastic hydrogels for interrogating pancreatic cancer-stromal cell interactions. *Materials Today Bio, 19*, 100576.

Liu, Q., Luo, Q., Ju, Y., & Song, G. (2020). Role of the mechanical microenvironment in cancer development and progression. *Cancer Biol Med, 17*(2), 282-292.

Lopez-Cavestany, M., Hahn, S. B., Hope, J. M., Reckhorn, N. T., Greenlee, J. D., Schwager, S. C., . . . King, M. R. (2023). Matrix stiffness induces epithelial-to-mesenchymal transition via Piezo1-regulated calcium flux in prostate cancer cells. *iScience, 26*(4), 106275. doi:10.1016/j.isci.2023.106275

Lopez, J., Kang, I., You, W., McDonald, D., & Weaver, V. (2011). *In Situ* force mapping of mammary gland transformation. *Integr. Biol (Camb), 3*(9), 910-921.

Markowski, M., Brown, A., & Barker, T. (2012). Directing epithelial to mesenchymal transition through engineered microenvironments displaying orthogonal adhesive and mechanical cues. *Journal of Biomedical Materials Research, 100A*(8), 2119-2127.

Marozas, I., Anseth, K., & Cooper-White, J. (2019). Adaptable boronate ester hydrogels with tunable viscoelastic spectra to probe timescale dependent mechanotransduction. *Biomaterials, 223*, 119430.

Martin, I., Nava, M., Wickström, S., & Gräter, F. (2022). ATP allosterically stabilizes integrin-linked kinase for efficient force generation. *Proceedings of the National Academy of the Sciences of the United States of America, 119*(11), e2106098119.

Massagué, J. (1998). TGF-β Signal Transduction. *Annu. Rev. Biochem., 67*, 753-791.

Massagué, J. (2008). TGFbeta in cancer. *Cell, 134*(2), 215-230.

McGrail, D. J., Kieu, Q. M., & Dawson, M. R. (2014). The malignancy of metastatic ovarian cancer cells is increased on soft matrices through a mechanosensitive Rho-ROCK pathway. *J Cell Sci, 127*(Pt 12), 2621-2626. doi:10.1242/jcs.144378

Morel, A., Liévre, M., Thomas, C., Hinkal, G., Ansieau, S., & Puisieux, A. (2008). Generation of breast cancer stem cells through epithelial-mesenchymal transition. *PLOS ONE, 3*(8), e2888.

Murrell, M., Kamm, R., & Matsudaira, P. (2011). Substrate viscosity enhances correlation in epithelial sheet movement. *Biophys J, 101*(2), 297-306. doi:10.1016/j.bpj.2011.05.048

Nalluri, S. M., O'Connor, J. W., & Gomez, E. W. (2015). Cytoskeletal signaling in TGFbeta-induced epithelial-mesenchymal transition. *Cytoskeleton (Hoboken), 72*(11), 557-569. doi:10.1002/cm.21263

Nelson, C. M., Khauv, D., Bissell, M. J., & Radisky, D. C. (2008). Change in cell shape is required for matrix metalloproteinase-induced epithelial-mesenchymal transition of mammary epithelial cells. *J Cell Biochem, 105*(1), 25-33. doi:10.1002/jcb.21821

O'Connor, J., & Gomez, E. (2013). Cell adhesion and shape regulate TGF-beta1-induced epithelial-myofibroblast transition via MRTF-A signaling. *PLOS ONE, 8*(12).

O'Connor, J., Riley, P. N., Nalluri, S. M., Ashar, P. K., & Gomez, E. W. (2015). Matrix rigidity mediates TGFβ1-induced epithelial-myofibroblast transition by controlling cytoskeletal organization and MRTF-A localization. *J. Cell Physiol., 230*, 1829-1839.

Pang, M., Siedlik, M., Han, S., Stallings-Mann, M., Radisky, D., & Nelson, C. (2016). Tissue Stiffness and Hypoxia Modulate the Integrin-Linked Kinase ILK to Control Breast Cancer Stem-like Cells. *Cancer Research, 76*(18), 5277-5287.

Pang, M., Teng, Y., Huang, J., Yuan, Y., Lin, F., & Xiong, C. (2017). Substrate stiffness promotes latent TGF-β1 activation in hepatocellular carcinoma. *Biochemical and Biophysical Research Communications, 483*(1), 553-558.

Plodinec, M., Loparic, M., Monnier, C., Obermann, E., Zanetti-Dallenbach, R., Oertle, P., . . . Schoenenberger, C. (2012). The nanomechanical signature of breast cancer. *nature nanotechnology, 7*, 757-765.

Rice, A. J., Cortes, E., Lachowski, D., Cheung, B. C. H., Karim, S. A., Morton, J. P., & Del Rio Hernandez, A. (2017). Matrix stiffness induces epithelial-mesenchymal transition and promotes chemoresistance in pancreatic cancer cells. *Oncogenesis, 6*(7), e352. doi:10.1038/oncsis.2017.54

Sankhe, C. S., Sacco, J. L., & Gomez, E. W. (2023). Biophysical Regulation of TGFβ Signaling in the Tumor Microenvironment. In I. Y. Wong & M. R. Dawson (Eds.), *Engineering and Physical Approaches to Cancer. Current Cancer Research.*: Springer, Cham.

Serrano, I., McDonald, P., & Dedhar, S. (2013). Role of integrin-linked kinase (ILK)/Rictor complex in TGFβ1-induced epithelial-mesenchymal transition (EMT). *Oncogene, 32*, 50-60.

Sharma, S., Goswami, R., Zhang, D., & Rahama, S. (2018). TRPV4 regulates matrix stiffness and TGFβ1-induced epithelial-mesenchymal transition. *Journal of Cellular and Molecular Medicine, 23*(2), 761-774.

Siegmann, K., Xydeas, T., Sinkus, R., Kraemer, B., Vogel, U., & Claussen, C. (2010). Diagnostic value of MR elastography in addition to contrast-enhanced MR imaging of the breast-initial clinical results. *European Radiology, 20*, 318-325.

Sinkus, R., Siegmann, K., Xydeas, T., Tanter, M., Claussen, C., & Fink, M. (2007). MR elastography of breast lesions: understanding the solid/liquid duality can improve the specificity of contrast-enhanced MR mammography. *Magnetic Resonance in Medicine, 58*(6), 1135-1144.

Stanchi, F., Grashoff, C., Nguemeni Yonga, C. F., Grall, D., Fassler, R., & Van Obberghen-Schilling, E. (2009). Molecular dissection of the ILK-PINCH-parvin triad reveals a fundamental role for the ILK kinase domain in the late stages of focal-adhesion maturation. *J Cell Sci, 122*(Pt 11), 1800-1811. doi:10.1242/jcs.044602

Tang, B., Vu, M., Booker, T., Santner, S., Miller, F., & Anver, M. (2003). TGF-beta switches from tumor suppressor to prometastatic factor in a model of breast cancer progression. *J. Clin. Invest., 112*(7), 1116-1124.

Tilghman, R., Cowan, C., Mih, J., Koryakina, Y., Gioeli, D., Slack-Davis, J., . . . Parsons, J. (2010). Matrix rigidity regulates cancer cell growth and cellular phenotype. *PLOS ONE, 5*(9), e12905.

Wang, H., Dembo, M., & Wang, Y. (2000). Substrate flexibility regulates growth and apoptosis of normal but not transformed cells. *American Journal of Physiology Cell Physiology, 279*, C1345-C1350.

Wei, S. C., Fattet, L., Tsai, J. H., Guo, Y., Pai, V. H., Majeski, H. E., . . . Yang, J. (2015). Matrix stiffness drives epithelial-mesenchymal transition and tumour metastasis through a TWIST1-G3BP2 mechanotransduction pathway. *Nat Cell Biol, 17*(5), 678-688. doi:10.1038/ncb3157

Wipff, P. J., Rifkin, D. B., Meister, J.-J., & Hinz, B. (2007). Myofibroblast contraction activates latent TGFβ1 from the extracellular matrix. *Journal of Cell Biology, 179*(6), 1311-1323.

Zervas, Y., Chen, K., Guo, L., & Wu, C. (2001). Drosophila integrin-linked kinase is required at sites of integrin adhesion to link the cytoskeleton to the plasma membrane. *Journal of Cell Biology, 152*, 1007-1018.

Figures

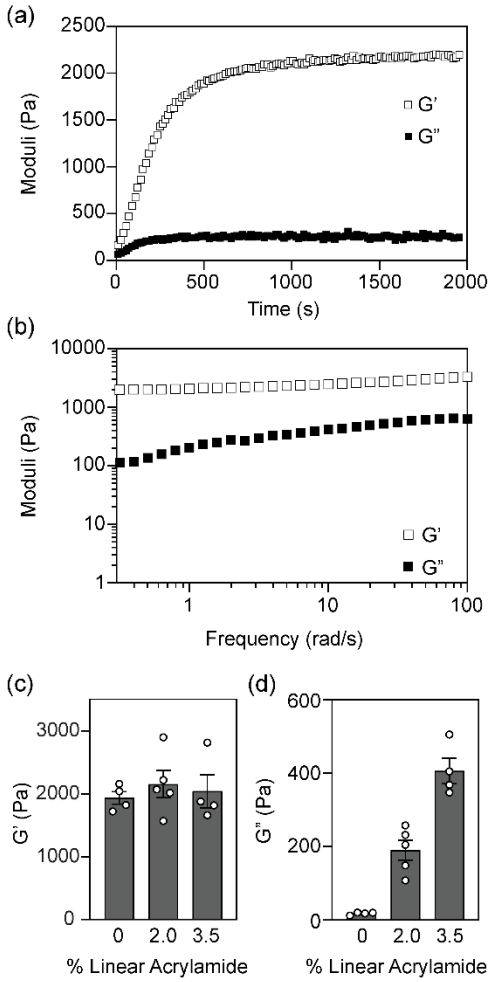

Figure 1. Mechanical characterization of viscoelastic polyacrylamide hydrogels. (a) Time sweep showing the storage (G') and loss (G") moduli as a hydrogel composed of 5% acrylamide, 0.1% bis-acrylamide, and 2.0% linear acrylamide polymerizes. (b) G' and G" as a function of frequency. Frequency sweep performed from 0.3-100 rad/s for the 2.0% linear acrylamide hydrogel. (c) G' and (d) G" as a function of w/v % linear acrylamide. Mechanical properties were measured at a frequency of 1 rad/s and 2% strain. Data represent the mean ± s.e.m. for $n \geq 3$.

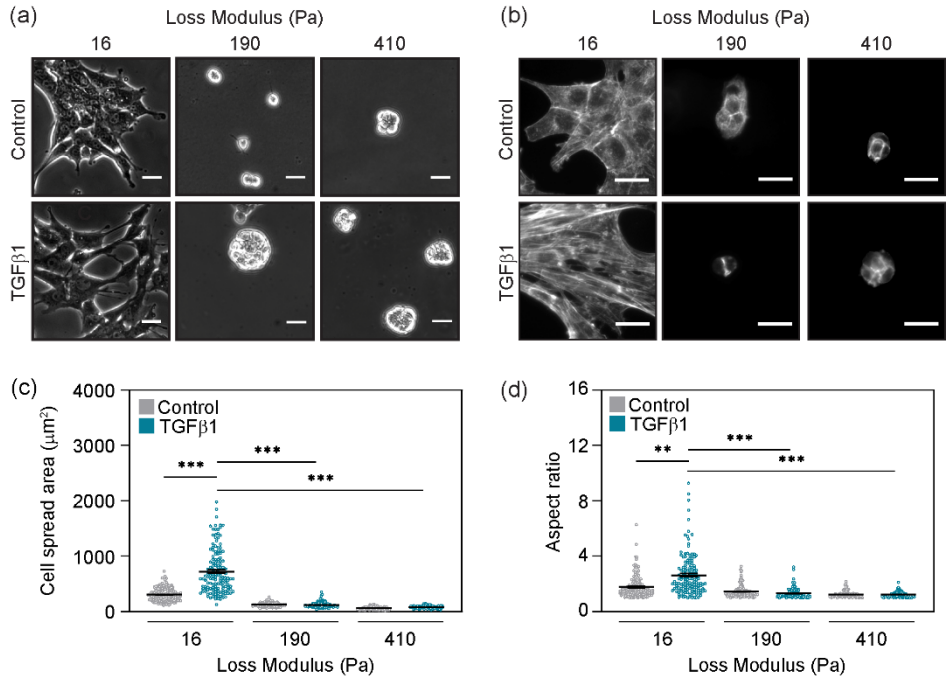

Figure 2. Substrate viscoelasticity regulates cell morphology and cytoskeletal organization in response to TGFβ1. (a) Phase contrast microscopy images of NMuMG cells cultured on hydrogels with G'=2000 Pa and varying G" and treated with TGFβ1 or a vehicle control. Scale bars: 25 μm. (b) Filamentous (F)-actin visualized with fluorescently tagged phalloidin. Scale bars: 25 μm. Quantification of cell (c) spread area and (d) aspect ratio from phase contrast images. Data are displayed as individual points with error bars representing mean ± s.e.m. with at least 150 cells analyzed over three different experiments; *p<0.05, **p<0.01, ***p<0.001.

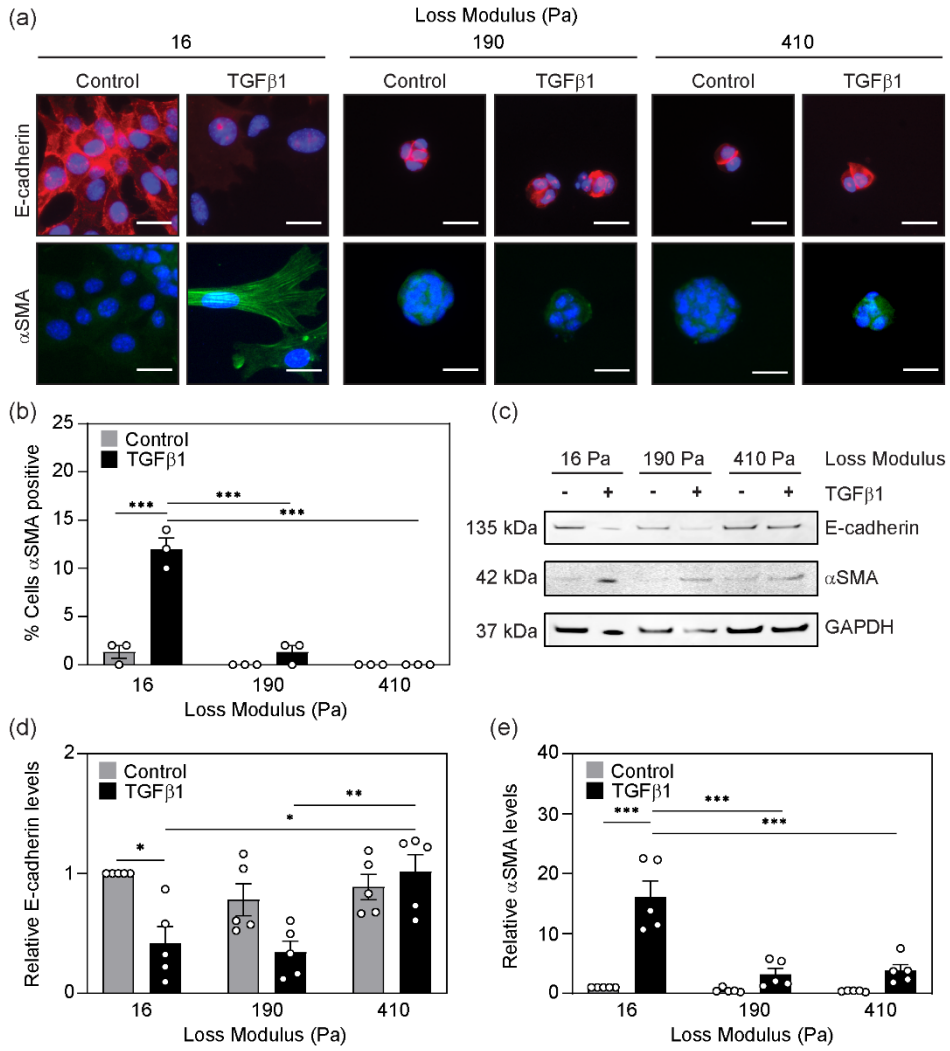

Figure 3. Increasing substrate loss modulus attenuates EMT-associated gene expression changes in response to TGFβ1. (a) Immunofluorescence staining images for the epithelial marker E-cadherin (red) and mesenchymal marker αSMA (green) in NMuMG cells cultured on hydrogels with G'=2000 Pa and varying G" and treated with TGFβ1 or a vehicle control for 48 hours. Cell nuclei are shown in blue. Scale bars: 25 μm. (b) Percentage of cells expressing αSMA. Data represent the mean ± s.e.m. for n=3 trials; ***p<0.001. (c) Western blot for E-cadherin and αSMA in cells cultured on viscoelastic substrates and treated with TGFβ1 or a vehicle control. Densitometric analysis quantifying relative (d) E-cadherin and (e) αSMA levels from western blots. Data represent the mean ± s.e.m. for n=5 trials; *p<0.05, **p<0.01, ***p<0.001.

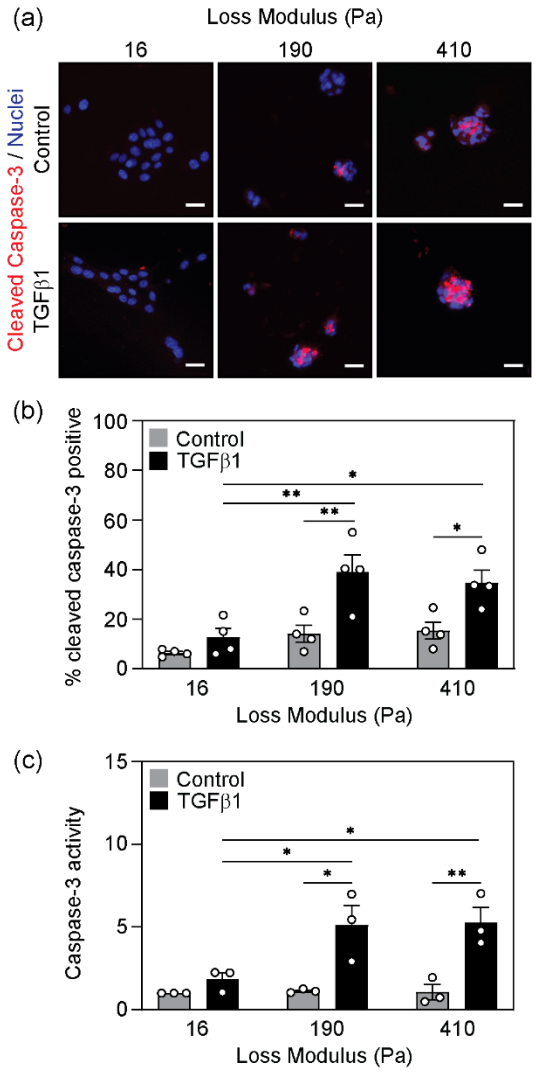

Figure 4. Increasing substrate viscoelasticity promotes TGFβ1-induced apoptosis. (a) Immunofluorescence staining for cleaved caspase-3 (red) and nuclei (blue) in NMuMG cells cultured on hydrogels with G'=2000 Pa and varying G" and treated with TGFβ1 or a vehicle control for 24 hours. Scale bars: 25 μm. (b) Percentage of cells expressing cleaved caspase-3. Data represent the mean ± s.e.m. for n=4 trials; *p<0.05, **p<0.01. (c) Cleaved caspase-3 activity in NMuMG cells cultured on hydrogels with G'=2000 Pa and varying G" and treated with TGFβ1 or a vehicle control for 24 hours. Data represent the mean ± s.e.m. for n=3; *p<0.05, **p<0.01.

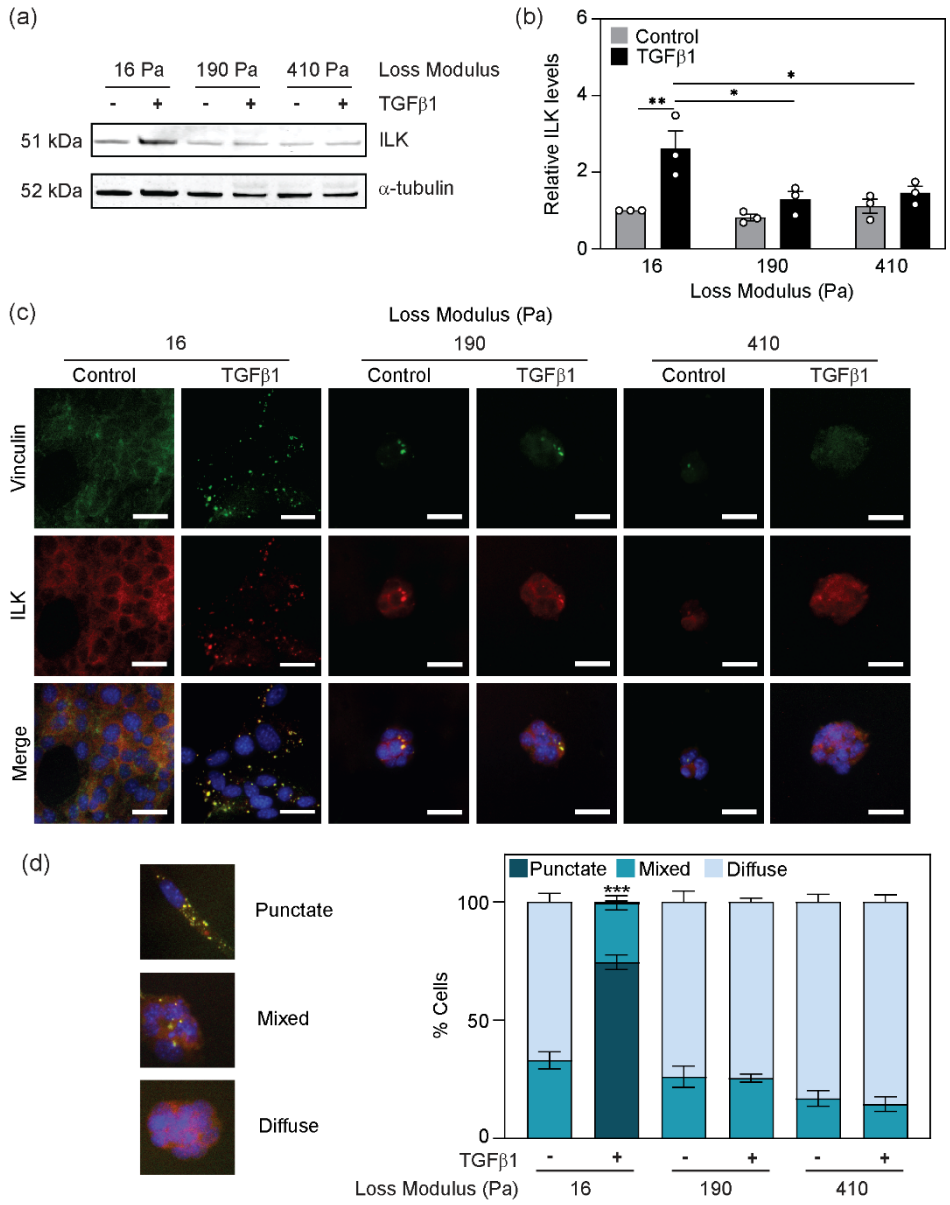

Figure 5. Matrix viscoelasticity and TGFβ1 regulate integrin linked kinase (ILK) expression and focal adhesion organization. (a) Western blot for ILK in NMuMG cells cultured on hydrogels with G'=2000 Pa and varying G" and treated with TGFβ1 or a vehicle control for 48 hours. (b) Densitometric analysis of western blot for relative ILK levels. Data represent the mean ± s.e.m. for n=3; *p<0.05; **p<0.01. (c) Immunofluorescence staining for vinculin (green) and ILK (red) in NMuMG cells cultured on hydrogels with G'=2000 Pa and varying G" and treated with TGFβ1 or a vehicle control for 48 hours. Cell nuclei are shown in blue. Merged images show co-localization of vinculin and ILK. Scale bars: 25 μm. (d) Percentage of cells showing vinculin and ILK organization characterized as punctate, mixed, or diffuse as indicated by the representative images. Data represent the mean ± s.e.m. for n=3; **p<0.001 compared to all other samples characterized as punctate.

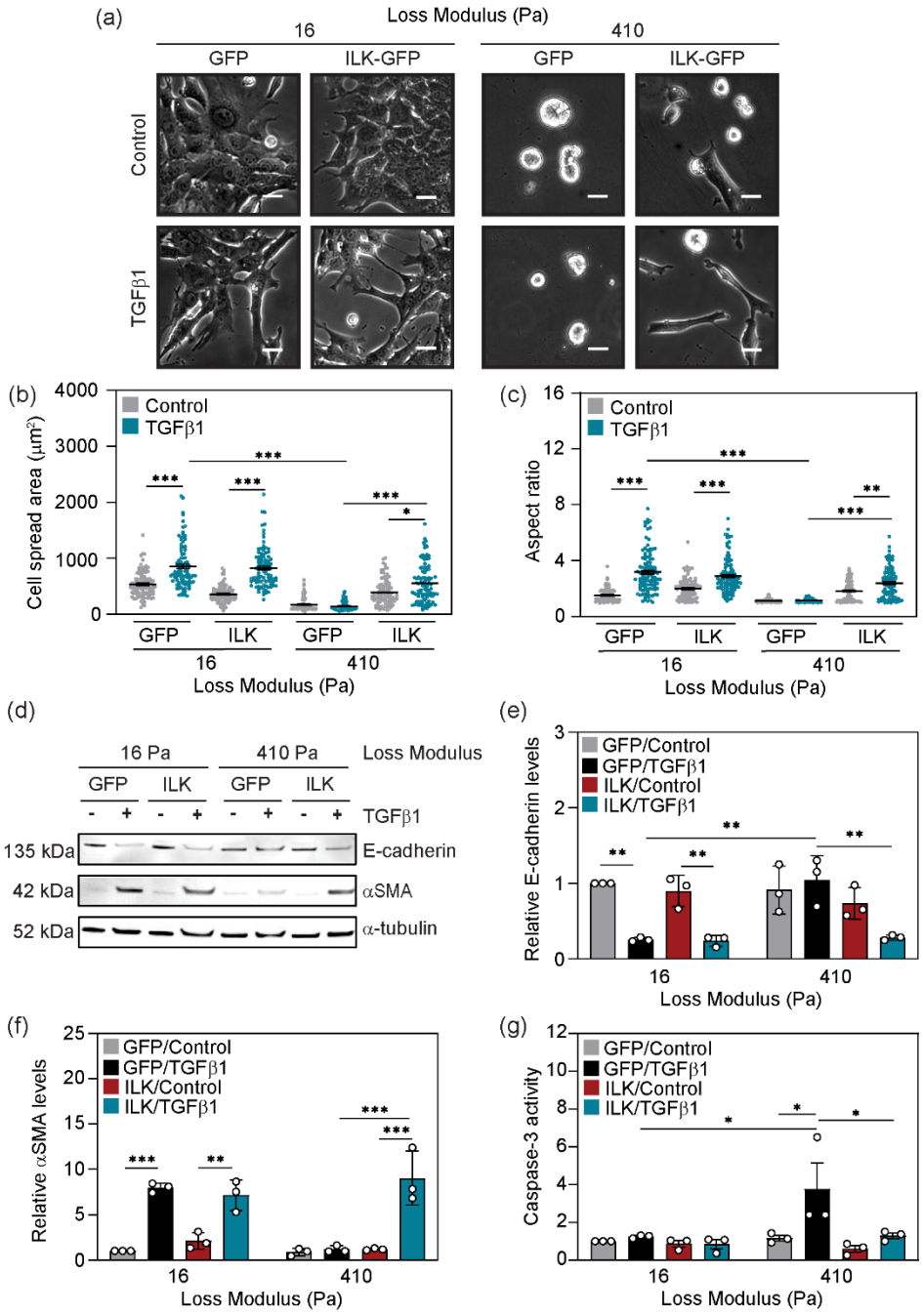

Figure 6. Integrin linked kinase (ILK) mediates cell response to TGFβ1 and viscoelasticity. (a) Phase contrast microscopy images of NMuMG cells cultured on hydrogels with G'=2000 Pa and varying G", transfected with a plasmid to overexpress ILK-GFP or a control GFP plasmid, and treated with TGFβ1 or a vehicle control for 48 hours. Scale bars: 25 μm. Quantification of cell (b) spread area and (c) aspect ratio from phase images shown in panel a. Data are displayed as individual points with error bars representing mean ± s.e.m. with at least 100 cells analyzed over three different experiments; *p<0.05, **p<0.01, ***p<0.001. (d) Western blot for E-cadherin and

αSMA in NMuMG cells cultured on hydrogels with G'=2000 Pa and varying G", transfected with a plasmid to overexpress ILK or a control GFP plasmid, and treated with TGFβ1 or a vehicle control for 48 hours. Densitometric analysis from western blots shown in panel d for relative levels of (e) E-cadherin, and (f) αSMA. Data represent the mean ± s.e.m. for n = 3; **$p<0.01$; ***$p<0.001$. (g) Cleaved caspase-3 activity in NMuMG cells cultured on hydrogels with G'=2000 Pa and varying G", transfected with a plasmid to overexpress ILK or a control GFP plasmid, and treated with TGFβ1 or a vehicle control for 24 hours. Data represent the mean ± s.e.m. for n = 3; *$p<0.05$.

Supporting Figures

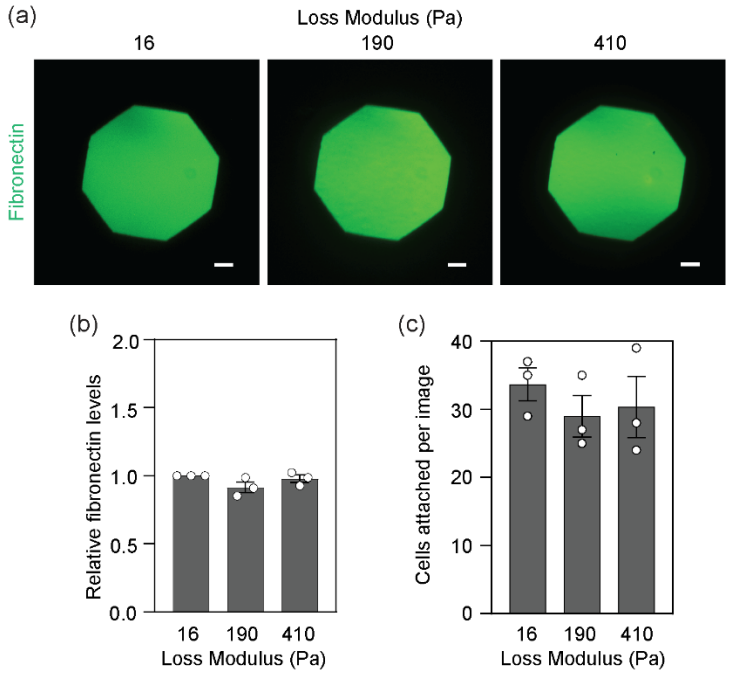

Figure S1. Fibronectin coating and cell attachment on viscoelastic hydrogel surfaces. (a) Immunofluorescence staining for fibronectin (green) on viscoelastic hydrogel surfaces. Scale bars: 25 μm. (b) Relative fibronectin levels as a function of matrix viscous dissipation. Data represent mean ± s.e.m. for n=3. (c) Number of NMuMG cells adhered to fibronectin-coated hydrogels of varying loss modulus 48 hours after plating across 3 separate phase images.

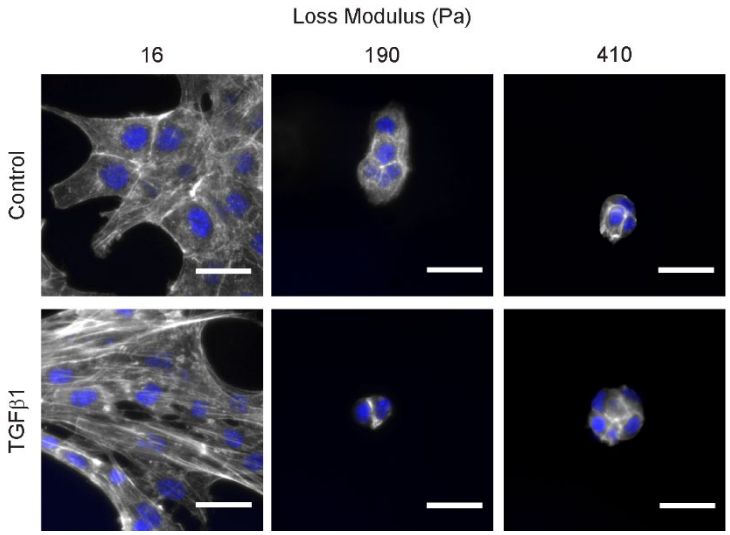

Figure S2. Filamentous (F)-actin visualized with fluorescently tagged phalloidin. Nuclei are shown in blue. Scale bars: 25 μm.

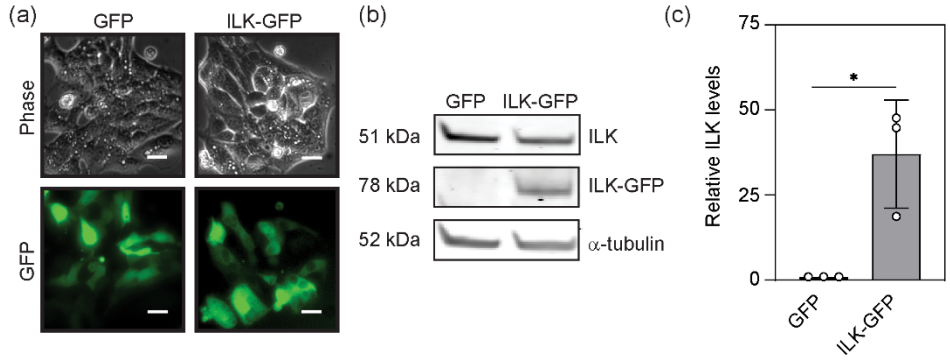

Figure S3. Transfection of cells with a mILK-GFP plasmid induces overexpression of ILK protein. (a) Phase and flourescence images of GFP and ILK-GFP transfected NMuMG cells cultured on tissue culture plastic. Images taken 24 hours after transfection. Scale bars: 25 μm. (b) Western blot for ILK and ILK-GFP from cells transfected with GFP and mILK-GFP plasmids and cultured on tissue culture plastic. (c) Densitometric analysis of relative ILK-GFP levels from western blot shown in panel b. Data represent mean ± s.e.m. for n=3; *$p<0.05$.